Fusion Engineering and Design 215 (2025) 115007

Contents lists available at ScienceDirect

Fusion Engineering and Design

journal homepage: www.elsevier.com/locate/fusengdes

Non-destructive ultrasonic inspections of small-scale mock-ups provided with advanced tungsten armours for DEMO divertor target

Riccardo De Luca [a,*], Emanuele Cacciotti [a], Marco Cerocchi [a], Francesco Crea [a], Selanna Roccella [a], Henri Greuner [b], Katja Hunger [b], Carsten Bonnekoh [c], Andrei Galatanu [d], Aljaž Iveković [e], Petra Jenuš [e], Marius Wirtz [f]

[a] ENEA, Nuclear Department, Via Enrico Fermi 45, 00044 Frascati, Rome, Italy
[b] Max Planck Institute for Plasma Physics, Boltzmannstr. 2, 85748 Garching, Germany
[c] Karlsruhe Institute of Technology, Institute for Applied Materials, Eggenstein-Leopoldshafen, Germany
[d] National Institute of Materials Physics (NIMP), Magurele 077125, Romania
[e] Department for Nanostructured Material, Jozef Stefan Institute, Ljubljana, Slovenia
[f] Forschungszentrum Jülich GmbH, Institute of Fusion Energy & Nuclear Waste Management –Plasmaphysik, 52425 Jülich, Germany

ARTICLE INFO

Keywords:
DEMO
Divertor
Advanced tungsten
High heat flux test
Non-destructive test
Ultrasonic examination

Within the framework of the EUROfusion Consortium, the Characterization of armour, heat sinks materials and joints sub-project of the Work Package Material (WP-MAT) has been dedicated to the development of different tungsten (W) monoblock mock-ups equipped with advanced materials for divertor target applications in the EU-DEMO fusion reactor. Assessing the status of the relevant joining interfaces of these mock-ups, not only after fabrication but throughout the whole component lifetime, plays a key role in the qualification process. At the ENEA Special Technologies Laboratory (TES), a number of facilities have been built to perform non-destructive inspections of plasma-facing components for fusion applications by ultrasonic testing (UT). The present work reports on the results of the UT inspections assessing the structural integrity of the relevant joining interfaces of three small-scale mock-ups provided with advanced W armour materials, specifically W-matrix with W_2C inclusions consolidated by Spark Plasma Sintering (SPS), K-doped rolled W and K-doped laminated W. The UT examinations are carried out after fabrication and after the high heat flux tests (HHFT) at the neutral beam facility GLADIS. All results confirm the high-quality joining achieved by HIP and HRP. During the HHF tests of mock-ups, after a few hundred HHFT cycles defects are detected at the joining interfaces, due to debonding, delamination and W material cracks mainly affecting the loaded zone. The ultrasonic pulse-echo technique provides not only the size and position of the defects in the plane orthogonal to the ultrasonic beam, but also their depth in the material. During the analysis, the probe is inserted inside the pipe and the mock-up is examined in a cylindrical configuration. The coupling medium (demineralized water) is poured only inside the pipe. The main inspection parameters and the piezoelectric probes are chosen to obtain the maximum resolution in accordance with the thickness and joining interfaces to be analyzed.

1. Introduction

Controlling the heat and particle exhaust in a tokamak is a key mission towards the realization of nuclear fusion [1]. In view of DEMO and future reactors, durable plasma-facing components (PFCs) are required, able to withstand the harsh operating conditions arising during plasma operation, i.e. high heat flux, erosion, sputtering as well as further limitations due to the presence of a consistent neutron irradiation [2]. In state-of-the-art PFCs, tungsten (W) is the preferred armor material owing to its high sputtering threshold, adequate thermophysical properties, low hydrogen retention and low activation [3]. However, it also shows unfavorable features for fusion applications [4–6], above all the fairly high ductile-to-brittle transition temperature (DBTT), even worsened by irradiation [7], and a pronounced recrystallization above 1300 °C. An active field of research within the EUROfusion workpackage "Material" (WP-MAT) regards the development of alternative advanced W materials as armours able to mitigate the intrinsic drawbacks of pure W. For instance, W-composites such as W-W laminates and W-fiber reinforced W [6] offer superior mechanical properties, pseudo-ductility and recrystallization resilience. W heavy

* Corresponding author.
E-mail address: riccardo.deluca@enea.it (R. De Luca).

https://doi.org/10.1016/j.fusengdes.2025.115007
Received 16 January 2025; Received in revised form 5 March 2025; Accepted 25 March 2025
Available online 30 March 2025

alloys such as W-2Y_2O_3 produced by Particle Injection Molding (PIM) [8] could be a cost-effective alternative with better recrystallization resilience, lower DBTT and, in some alloys, self-passivating features. Dispersion strengthened/stabilized W materials such as K-doped W (cold-rolled or laminated) [9] and W with W_2C inclusions consolidated by means of Field Assisted Sintering Technique (FAST) or Spark Plasma Sintering (SPS) processes [10] are also an option, owing to their high recrystallization resilience and superior strength with reduced worsening under neutron irradiation.

In the context of the necessary qualification of innovative armour materials, small-scale mock-ups equipped with advanced monoblocks have been fabricated by means of hot isostatic pressing (HIP) [11] or hot radial pressing (HRP) [12]. In particular, the HIP cycle consists of a first stage at 550 °C and 100 MPa argon pressure for 4 h, followed by a second stage at 450 °C for 1 h, during which the argon pressure is kept constant at 100 MPa [11]. After the fabrication, these mock-ups have been tested. Above all, the cyclic thermal fatigue behavior is assessed at the neutral beam facility GLADIS [13] up to several hundred cycles at 20MW/m^2 and hot water cooling conditions (16m/s, 130 °C, 4 MPa). Non-destructive testing (NDT) plays a key role, as it helps assess the integrity of the relevant joining interfaces of a mock-up multiple times throughout its lifetime, without altering its functionality hence the possibility to perform additional tests. With respect to other NDT techniques, above all neutron tomography [14], X-Ray tomography [15] and laser thermography [16], the UT method is relatively simple and inexpensive, so it is currently one of the most widely employed methods in fusion applications. At the ENEA Special Technologies Laboratory (TES), a number of facilities have been built to perform non-destructive inspections of small-scale mock-ups and components by ultrasonic testing (UT). The ultrasonic pulse-echo water gap technique provides not only the size and position of the defects in the plane orthogonal to the ultrasonic beam, but also their depth in the material. Many papers are available on the UT examinations carried out on mock-ups for nuclear fusion applications [17,18]. In all cases, the main focus is on the investigation of different target design solutions that always rely on pure W as armour material. On the contrary, little to no literature is available on the use of UT in support of the development of potential alternatives to pure W in view of the EU-DEMO and future reactors.

In the present work, the results of the UT inspections carried out on three small-scale mock-ups provided with advanced monoblocks made of innovative armour materials, i.e. W alloys and W composites, are described. The results obtained helped assess the impact of the high heat flux tests (HHFT) on the structural integrity of the relevant joining interfaces. The three mock-ups analyzed in this work are shown in Fig. 1 together with the orientation of the measurement axis. In detail:

a) **ENEA80**: manufactured by ENEA by means of HRP technique and equipped with four K-doped W laminates monoblocks (flagged with IDs 62–58–54–52) provided by the National Institute of Materials Physics (NIMP) [9]. Each monoblock consists of 120 laminae joined together, for a total thickness of 12mm. The layout of each monoblock reflects the same geometry of the DEMO-like divertor target W-monoblock [19]. In detail, it consists of a CuCrZr cooling pipe with an inner diameter of 12 mm and thickness of 1 .5mm. The pipe is bonded to 23 × 28 × 12 mm W-blocks through a Cu interlayer having a thickness of 1 mm and outer diameter of 17mm. UT inspections were carried out after fabrication and at two steps of the HHFT campaign, respectively after 1500 and 2000 cycles at 20MW/m^2

b) **MU II - IJS**: manufactured by means of HIP technique and equipped with three W-W_2C (4 %wt. of W_2C) monoblocks realized by the Department for Nanostructured Material Jozef Stefan Institute (IJS). Their position in the mock-up layout of Fig. 1b is 4–5–6, respectively. Each of them has an axial thickness of 4mm. The other geometrical features of each monoblock reflect those of the above-mentioned DEMO-like divertor target W-monoblock design. UT inspections were carried out after fabrication and after 500 × 20MW/m^2 cycles

c) **MU III - Tohoku**: manufactured by means of HIP technique and equipped with four K-doped rolled W monoblocks provided by the Tohoku University in Japan [11]. Also in this case, the DEMO-like divertor target design is chosen, except for the axial thickness, equal to 4mm. In the mock-up layout of Fig. 1c the advanced W monoblocks are located at the positions 4–5–8–9. UT inspections were carried out after fabrication and after 500 × 20MW/m^2 cycles

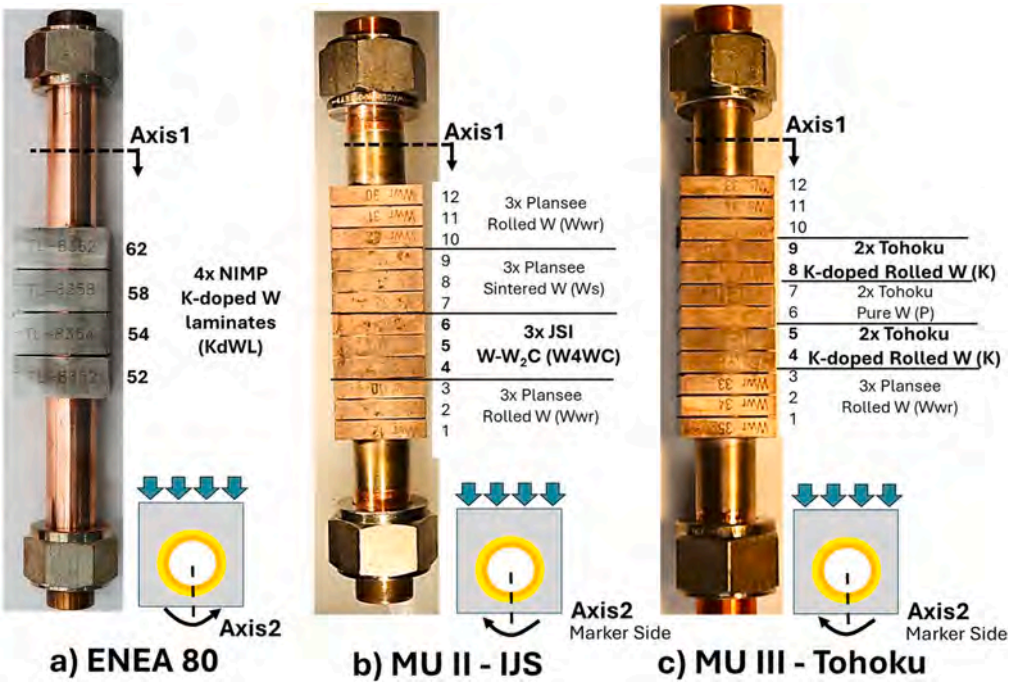

Fig. 1. Inspected mock-ups and measurement axis orientation: a) ENEA80, a mock-up consisting of 4 K-doped W laminates monoblocks provided by NIMP; b) MU II – IJS, a mock-up containing three W-W_2C monoblocks provided by IJS; c) MU III – Tohoku, equipped with four K-doped rolled W monoblocks.

2. UT equipment and setup

The UT equipment is shown on the right side of Fig. 2. It is based on the pulse/echo technique in demineralized water, the coupling medium. A piezoelectric probe specifically developed by General Electric for this application, works as pulser and receiver. A Karl Deutch Ecograph provides the pulse trigger and sets the signal amplification (in dB) and acquisition rate. A step-motor-driven motion system ensures up to 4 degrees of freedom to perform planar or cylindrical inspections with a very high spatial resolution. For the particular application, i.e. for the radial inspection from the inside of pipes having an inner diameter of 12 mm, a compact piezoelectric probe with focalized beam was specifically developed [20]. It is characterized by a single lateral element with an effective diameter of 3 mm, focal length in water of 7.6 mm and operating frequency of 15MHz. As shown in the technical drawing of Fig. 2, the probe is inserted inside a cylindrical holder specifically designed to ensure the correct alignment and spacing between the probe and the inner surface of the pipe. In the present work, demineralized water is poured only inside the pipe. This solution helps keep unaltered the status and the chemical composition of the external surfaces of the mock-up, and especially the emissivity of the plasma facing side will not be affected. Cylindrical inspections are carried out by moving the probe inside the pipe according to a cylindrical grid with optimized spatial resolution of 0.08 mm x 1° (respectively, Axis1 and Axis 2 in Fig. 1). The signal is acquired at every node of the measurement grid (point measure) during the axial translation. The zero of the axis2 is conventionally chosen at the center of the low heat flux side (opposite to the loaded side). Consequently, the loaded side is always delimited by the range 145–215°

The acquired data are then processed and analyzed in detail. The results can be visualized in the form of:

1. **A-scan**: "raw" signal acquired over time at a single point measure. At a given sound speed, time can be easily converted into depth (in mm). The sound speed of longitudinal waves propagating at room temperature (20 °C) in the analyzed materials was employed. It is similar for Cu and CuCrZr, and equal to 4900m/s [18]. The sound speed of the advanced W materials was preliminary assessed through UT examinations of small samples with a known thickness. The results suggest that their sound speed at room temperature is not much different from that of pure W, so the value 5200m/s was also employed for the advanced W materials. As a future step, reference blocks with artificial defects will be fabricated for each advanced W material. They will be used for a more accurate calibration of the measurement system. In addition, the signal amplitude is provided as a percentage of the Full-Screen (%FS) amplitude, namely related to a characteristic value of the employed echograph. This choice is aimed at preserving the similarity between measurements acquired with the same echograph but with different probes and mock-ups.
2. **C-scan**: map visualization of the measurement grid, where each pixel (point measure) has a color that is given by the maximum signal amplitude within a user-defined time-of-flight (ToF) or depth window. The amplitude of the signal is expressed in %FS.
3. **D-scan**: similar to the C-scan, but with color code given by the ToF value corresponding to the maximum signal amplitude within a ToF or depth window.
4. **B-scan:** plot of A-scans along a vertical path of a C-scan, with colors given by the signal amplitude

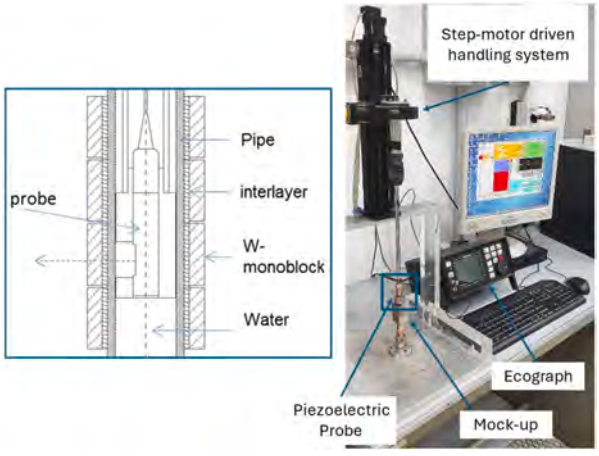

Fig. 2. The employed UT equipment with an axial cross section drawing of the mock-up, showing the probe holder inside the pipe, which ensures the correct probe alignment.

An important step before starting each measurement session is the UT system calibration, well described in [20]. If available, calibration blocks with reference holes can be employed at this stage. Above all, the amplification of the echograph (or gain, in dB) is adjusted in order to have the signal of a reference interface at a reference value, for instance 80 %FS. The reference interface can be, for instance, the first interface (water/CuCrZr interface) or the "naked pipe" signal detected at the depth of the CuCrZr/Cu interface. A more detailed description of the UT equipment, measurement setup, calibration and data visualization options can be found in published papers [17,20].

3. ENEA80 (K-doped W laminates) UT results

The UT results related to the CuCrZr/Cu interface of ENEA80 are reported in c. The C-scan maps show the status after fabrication (a) and after 1500 HHFT cycles at 20MW/m^2 (b). The blue areas in the C-scan indicate the absence of discontinuities in the material. The C-Scan after fabrication (Fig. 3a) suggests high-quality joining obtained by HRP, with almost no indication of discontinuities in the four monoblocks. Instead, in the C-scan of Fig. 3b indications of discontinuities are detected after 1500 cycles, located at the edges of the monoblocks in the loaded zone. Defects at the CuCrZr/Cu interface are likely due to debonding and delamination. The first type is originated by a detachment between two different materials at their joining interface. Consequently, this defect is predominantly elongated in the circumferential direction rather than in the radial direction (depth). As reported in Fig. 3b, in ENEA80 debonding is more pronounced at the ends of the mock-up, with a total detached area of 48.7mm^2 on the left side of monoblock #62 (defect ID:

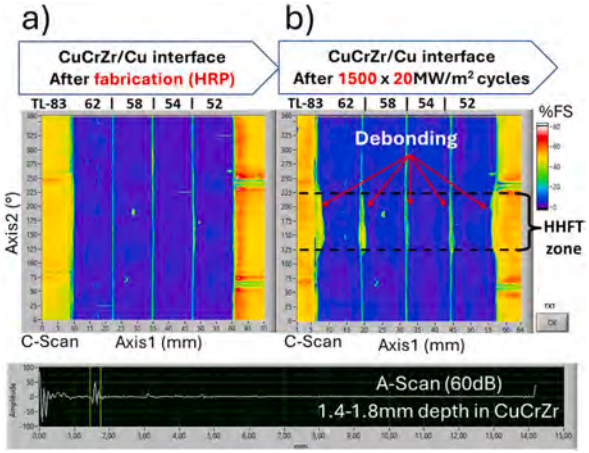

Fig. 3. ENEA80 CuCrZr/Cu joining interface. The A-Scan show the "raw" signal at a point measure on the "naked pipe" and the depth range in CuCrZr (ToF window) to which the C-scans are related. The C-scan maps show the status of the interface after fabrication a) and after 1500 × 20MW/m^2 HHFT cycles b). The black dotted lines delimit the high heat flux side, called "HHFT zone". In the C-scan map, the blue color indicates a well attached joining interface.

1) and 18.2mm^2 on the right side monoblock #52 (defect ID: 3). Moving towards the center this issue becomes less pronounced. This phenomenon could be related to the deformation due to the bending of the pipe during cyclic thermal fatigue tests. However, the main causes are still unclear and further studies are required. Unlike debonding, delamination is usually related to the presence of discontinuities in the radial direction, for instance deep cracks propagating through the monoblock up to reaching to the underlying joining interfaces. For instance, in ENEA80 a detachment between adjacent K-doped W laminae could lead to delamination defects. This type of defect is usually hard to detect with radial UT inspections.

Fig. 4 and Fig. 5 show respectively the status of the CuCrZr/Cu interface and Cu/W interface after the additional 500 cycle, thus after the completion of 2000 cycles in total. The black dotted lines delimit the loaded zone, i.e. the high heat flux side, which is contained in the range 125°−225° in the DEMO-like W-monoblock design. Interestingly, the discontinuities already detected after 1500 cycles appear only marginally worsened. The same conclusion is also valid for the Cu/W interface, shown in Fig. 5. Here the greatest defect is on monoblock #52, with an overall detachment of 16.6mm^2 (defect ID: 9). This suggests that near all the detected discontinuities formed at the initial phase of the HHFT, without further worsening during the additional 500 cycles. At the Cu/W interface, the discontinuities look compatible with debonding and delamination. The latter mechanism characterizes defects that are predominantly elongated in the circumferential direction; therefore, they could be likely due to the detachment of W laminae.

In this context, a preliminary defect sizing was carried out using the same procedure established for the ITER-like W-monoblock design [20]. This provides a very accurate assessment of the defects at the CuCrZr/Cu interface. Instead, for the Cu/W joining interface and beyond, a calibration of the measurement system would be required, ideally using a reference block with artificial defects for each advanced W material. The fabrication of reference blocks is currently foreseen, but it is not yet accomplished. Therefore, at this preliminary stage it was assumed that dense W and advanced W materials share the same behavior, as suggested by preliminary UT inspections. An originally developed software was employed in this context [20], and the results obtained are summarized in Table 1. After having selected the joining interface and a proper defect amplitude threshold, the user can draw a box around a defect to be sized. The dimensions of the bounding box are reported in Table 1 as ΔAxis1 and ΔAxis2. Each node of the measurement grid contained in the bounding box selection is analyzed. Above all, the software calculates with high accuracy the defect distance R with respect

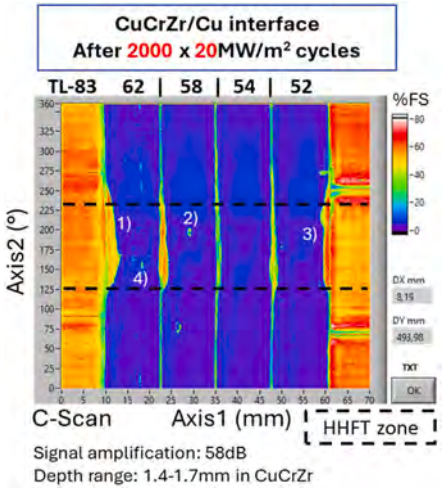

Fig. 4. CuCrZr/Cu joining interface of ENEA80 after 2000 × 20MW/m^2 HHFT cycles (1.4–1.7 mm depth range in CuCrZr). The Defects flagged with IDs were analyzed in detail and sized.

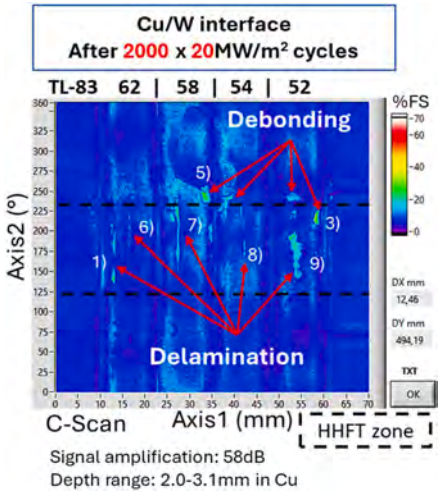

Fig. 5. Cu/W joining interface of ENEA80 after 2000 × 20MW/m^2 HHFT cycles (2.0–3.1 mm depth range in Cu). Defects flagged with IDs were analyzed in detail and sized.

Table 1
Defect sizing.

ID	Interface	ΔAxis1 (mm)	ΔAxis2 (°)	Area (mm^2)	Detected after
1)	CuCrZr/Cu*	4.08	168	48.76	1500 cycles
2)	CuCrZr/Cu	0.72	10	0.41	Fabrication
3)	CuCrZr/Cu*	1.76	133	18.21	1500 cycles
4)	CuCrZr/Cu	0.56	9	0.42	2000 cycles
5)	Cu/W	1.52	24	2.50	1500 cycles
6)	Cu/W**	0.5	86	6.43	1500 cycles
7)	Cu/W**	1.04	85	3.52	1500 cycles
8)	Cu/W**	1.12	69	1.65	1500 cycles
9)	Cu/W**	3.28	57	16.65	1500 cycles
10)	W**	8.16	30	22.95	1500 cycles

* Defect extending up to the Cu/W interface.
** Delamination reaching the outer surface of the monoblock.

to the pipe axis and the fraction f between the nodes with signal amplitude beyond the defect threshold ("defect nodes") and the total number of nodes contained in the bounding box. Finally, the area of the defect is derived from the area of the bounding box, as follows:

$$A = \Delta\text{Axis1}\cdot\Delta\text{Axis2}\frac{\pi}{180}R\cdot f \quad (1)$$

The D-scan in Fig. 6a shows the backwall echoes reflected from the external sides of the monoblocks. Detecting the characteristic backwall echo signals is a valuable indication of the absence of discontinuities, which would hinder the propagation of the acoustic wave up to the external surfaces of the monoblock. The colours in the D-scan reflect the geometry of the DEMO-like W-monoblock [19], i.e. three sides with 3 mm W thickness and 8 mm armour thicknes on the high heat flux side. Lacks in the backwall echo signals are visible in Fig. 6a, likely due to the presence of delaminations affecting the monoblocks #52–54–58 (defect ID: 7–8–9). Such discontinuities propagate radially towards the Cu/W interface and, in severe cases, can even reach it, as suggested by in the C-scan of Fig. 5. In addition to delamination, an axial crack (defect ID: 10) formed on monoblock #62 around 125° along axis2. Its morphology and depth were assessed by analyzing the point measures along a circumferential path (red dotted path in Fig. 6a). The resulting B-scan is reported in Fig. 6b The crack starts on the lateral side, then it propagates straight towards the tested zone covering a circumferential angle of 30°, from 115° to 140°. It nearly stops at the beginning of the loaded zone. In terms of depth, it stops around 1–2 mm from the Cu/W interface.

The post-mortem metallographic examination of ENEA80 was

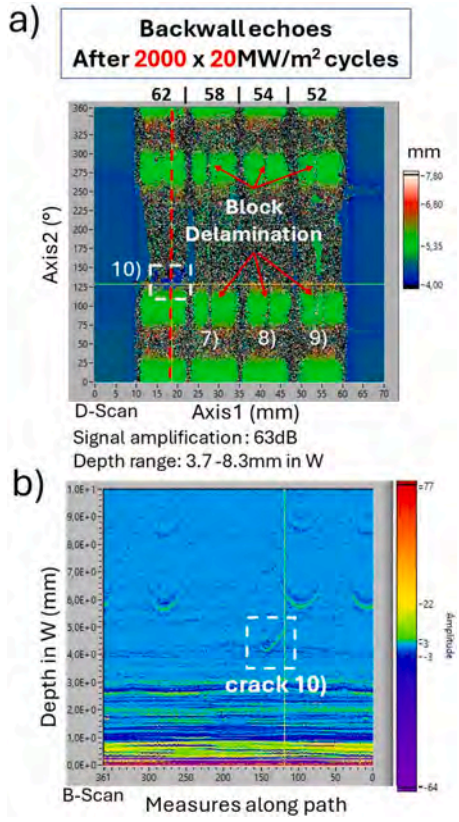

Fig. 6. Delamination and cracks affecting ENEA80. a) D-scan map (3.7–8.3 mm depth range in W) highlighting discontinuities in the blocks. Voids in the backwall echoes of the three shorter sides of the monoblocks suggest the presence of discontinuities. b) The point measures along the red dotted path are analyzed in a B-Scan. In addition to the backwall echo signals, a crack is detected on monoblock #62 at a depth range of 1–2 mm from the Cu/W interface and circumferential extension of 30°.

carried out at the Max Planck Institute for Plasma Physics (IPP) of Garching with the goal of providing a final validation of the main findings of the UT inspection. The cutting scheme was defined based on the position of the main discontinuities detected by UT. As shown in Fig. 7, the presence of delamination on the monoblocks #52–54–58 is confirmed (defect ID: 7–8–9). It was also confirmed that they reach the Cu/W interface. Even the small defects highlighted in the gaps between these monoblocks could be likely related to the debonding detected by UT after HHFT at the CuCrZr/Cu interface. Fig. 8 shows the transversal cut view of monoblock #62. With respect to the axial crack on the lateral side, very good agreement was confirmed with respect to the morphology and depth outlined by the detailed UT analysis. A small detachment is also observed at the CuCrZr/Cu interface, around 150°. It looks compatible with the discontinuity detected after 2000 cycles at the center of the HHFT zone of monoblock #62, (defect ID: 4). A detailed description of the findings of the post-mortem examination will be provided in a dedicated publication. Some defects are also visible to the naked eye on the outer surfaces of the mock-up (as shown in Fig. 7 and Fig. 8).

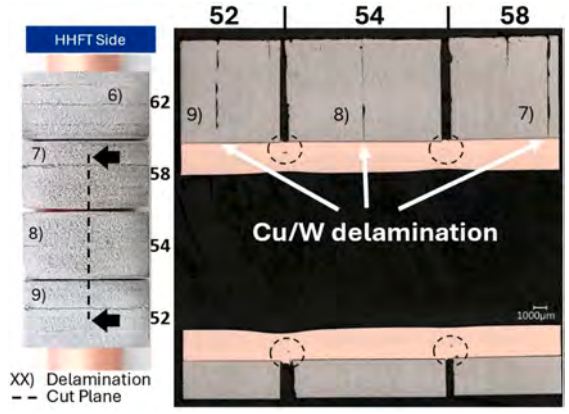

Fig. 7. Metallographic examination of monoblocks #52–54–58 (axial cut) in support of the UT result, confirming delamination up to the Cu/W interface and debonding in the gaps at the CuCrZr/Cu interface. These results indicate that delamination 7), 8) and 9) run across the monoblock up to reaching the Cu/W interface.

4. MU II - IJS (W-W_2C) UT results

The D-Scans of Fig. 9 show the backwall echoes of the mock-up MU II – IJS after fabrication (Fig. 9a) and after the HHFT tests (Fig. 9b), which consisted of 500 HHFT cycles at 20MW/m^2. In the D-scan, the echoes from the external faces of each monoblock appear as bands. In particular, the red band is the echo reflected by the HHFT surface, whereas the other bands have a different color as they refer to the other three sides of the block with lower thickness of W. The results after fabrication suggest good quality joining obtained by the HIP process, confirming the suitability of this fabrication process. The presence of voids in the backwall echo signals may indicate the presence of discontinuities that prevent the sound from propagating up to the external surfaces of the monoblock. As shown in the D-Scan of Fig. 9b, this seems to be the case: the echo from the HHFT side is not visible in the loaded zone of monoblocks from #4 to #9. A more detailed UT analysis, also supported by visual inspections, suggests indeed the presence of defects, as described hereafter.

With respect to the advanced W monoblocks in position 4–5–6, the C-Scan in Fig. 10 shows the formation of clustered defects in the loaded zone, with a circumferential extension up to 75° on monoblock #4. However, their dimension does not justify the complete absence of the backwall echo in that area. Therefore, the presence of further discontinuities is highly probable, although not confirmed in the present examination. With respect to the sintered monoblocks in position 7–8–9, a large detachment formed at the W/Cu interface, as highlighted in the C-Scan of Fig. 11. This defect affects almost completely the tested zone of monoblocks #8 and #9, having a total extension of 25 mm along axis1 and 150° on axis2 (from 125° to 275°). Further investigations were carried out by analyzing the point measures along three circumferential paths (the red dotted lines in Fig. 11). The resulting B-scan visualizations

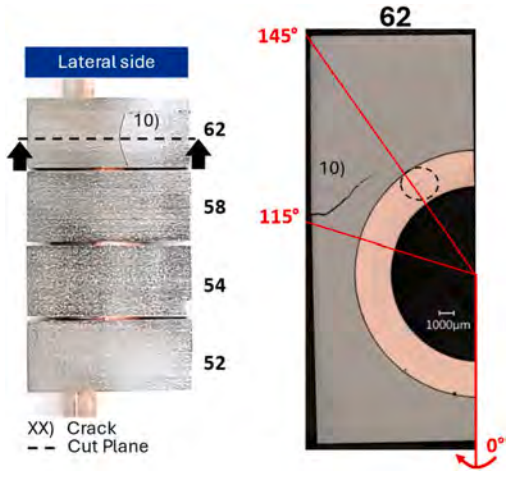

Fig. 8. Metallographic examination of monoblock #62 (transversal cut) to verify the morphology and depth of the axial crack 10).

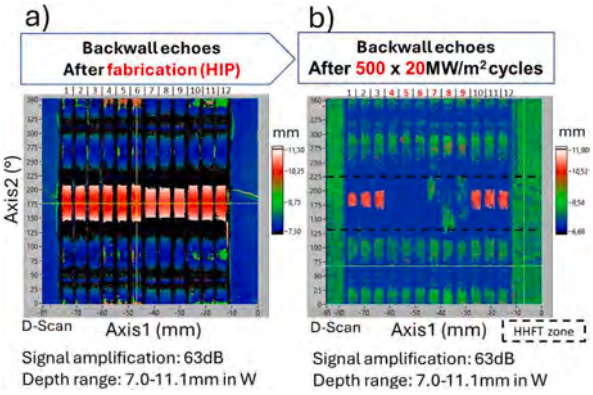

Fig. 9. Backwall echoes of MU II – IJS (7.0–11.0 mm depth in W) reported after fabrication a) and after 500 × 20MW/m^2 HHFT cycles b). In the D-scan, the backwall echoes appear like bands, and the echo from the HHFT side is the red one around 180. The different colors reflect the different block thicknesses. A lack of signal in the backwall echoes may indicate the presence of discontinuities hindering the propagation of the acoustic wave.

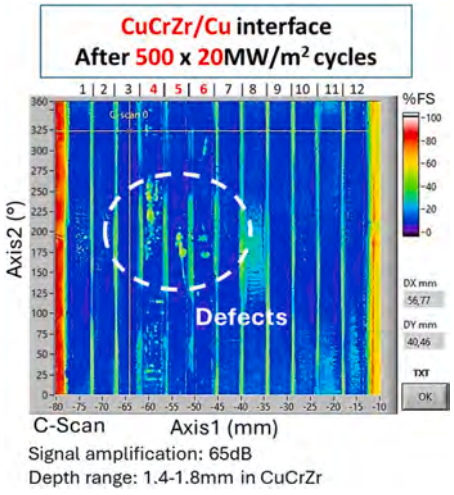

Fig. 10. CuCrZr/Cu joining interface of MU II -IJS after 500 × 20MW/m^2 cycles. The presence of clustered discontinuities on monoblock #4–5–6 is highlighted in the C-scan (1.4–1.8 mm depth range in CuCrZr).

are reported in Fig. 12a, Fig. 12c and Fig. 12e. The B-scans provide useful information on the depth and morphology of this large discontinuity. It turned out that such a large defect is connected to cracks in the sintered W monoblocks. They run almost circumferentially for about 50° at a depth of 2–2.5 mm from the first interface, before departing towards the external surfaces. A further confirmation is provided by visual inspection, as shown in Fig. 12b, Fig. 12d and Fig. 12f, which refer to monoblocks #7–8–9, respectively. Axial cracks are visible on the external surfaces of these monoblocks at the position where UT indicated the presence of discontinuities.

5. MU III - Tohoku (K-doped rolled W) UT results

The C-Scan in Fig. 13a provides a clear indication of the quality of the joining produced by the HIP process between the CuCrZr pipe and the Cu interlayer. The overall absence of defects after fabrication makes even more evident the impact of the cyclic thermal fatigue on this mock-up. The C-scan of the CuCrZr/Cu interface after 500 × 20MW/m^2 cycles (Fig. 13b) reveals two discontinuities at the edges of the monoblocks #9 and #11. As shown in Fig. 13b, their shape seems compatible with a localized debonding near the edges of monoblock #10. It affects the

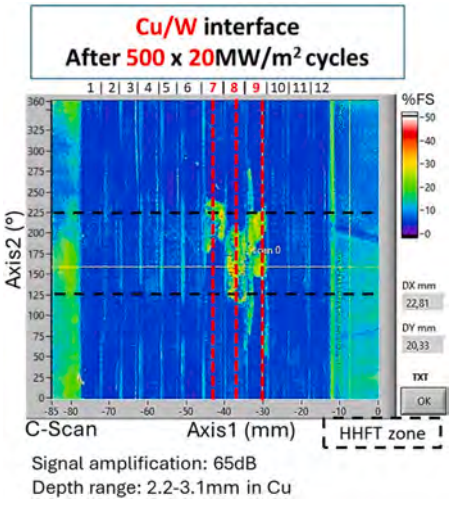

Fig. 11. Cu/W joining interface of MU II -IJS after 500 × 20MW/m^2 cycles (2.2–3.1 mm depth range in Cu). A large discontinuity affects the loaded zone of monoblocks #7–8–9. The red dotted lines are circumferential paths used for a more detailed investigation of the morphology and depth of the defect.

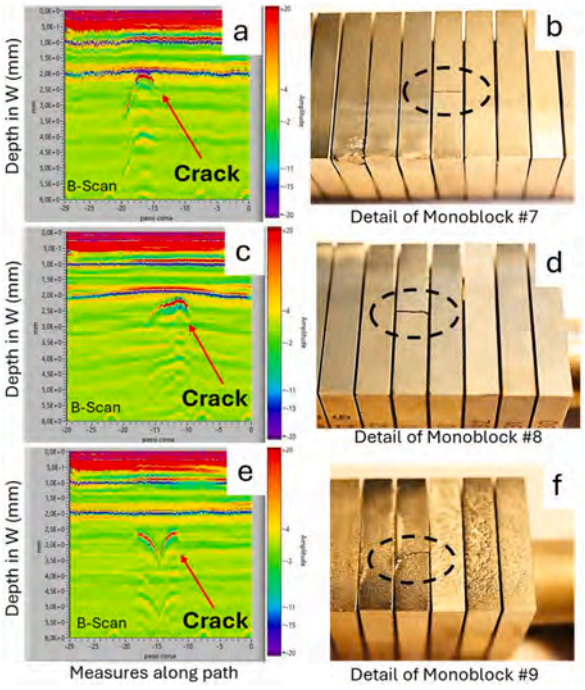

Fig. 12. Detailed crack analysis of MU II – IJS. a), c) and e) are the B-scan resulting from the analysis of all the point measures along three circumferential paths, respectively on monoblocks #7–8–9. Results indicate that these discontinuities are related to cracks in the monoblocks. b), d) and f) are pictures from the visual inspection confirming the presence of cracks on these monoblocks.

whole tested zone in the circumferential direction, i.e. from −125 to −225°, but only a few mm in the axial direction. Monoblock #10 does not show visible indications of defects at this interface. However, further analysis revealed the presence of a large detachment at the Cu/W interface of monoblock #10, as shown in the C-scan of Fig. 14a. The B-scan in Fig. 14b represents the point measures along the red dotted line drawn in Fig. 14b. It suggests that the above-mentioned discontinuities are likely interlinked. In addition, they could be related to the presence of a deep crack in the W block, running from the Cu/W interaface up to a depth of approximately 2 mm in W. Visual inspection in Fig. 14c

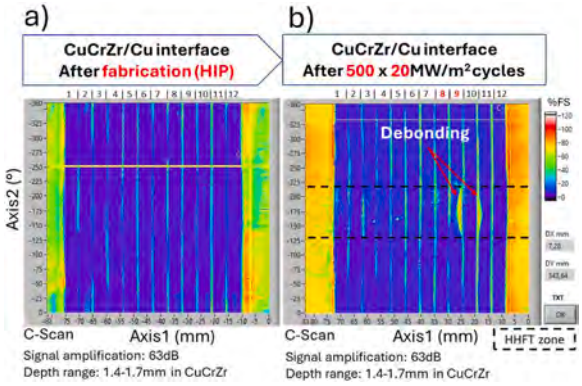

Fig. 13. CuCrZr/Cu interface of MU III – Tohoku (1.4–1.7 mm depth range in CuCrZr) after fabrication a) and after 500 × 20MW/m^2 HHFT cycles b). The high quality of the joining interface produced by means of HIP process can be noticed. After the tests, a localized discontinuity formed at the edges of monoblocks #9 and #11.

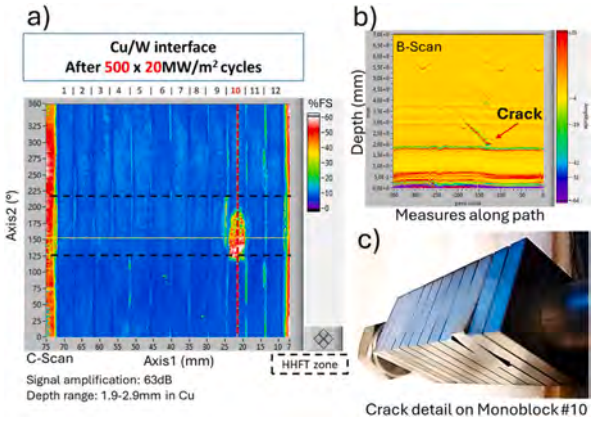

Fig. 14. Detailed analysis of cracks on the monoblock #10 MU III – Tohoku. a) C-scan revealing a large defect formed after the tests at the Cu/W interface (1.9–2.9 mm depth range in Cu). b) B-Scan analysis of the measures along the red path, suggesting that the discontinuity is likely a crack in the block, propagating from the external surface up to a depth of 2mm. c) Detail from visual inspection, in support of the UT results.

suggests that the crack propagates up to the external surfaces, with a visible deformation of the W block.

6. Conclusions

In support of the EUROfusion WPMAT research program, three mock-ups provided with advanced W monoblocks have been analyzed by means of non-destructive ultrasonic examinations. The analyzed mock-ups are: ENEA80, manufactured by ENEA by means of HRP and equipped with four K-doped W laminates monoblocks provided by NIMP; MU II - IJS, manufactured by means of HIP technique and equipped with three W-W_2C (4 %wt. of W_2C) monoblocks provided by IJS and MU III - Tohoku, manufactured by means of HIP technique and equipped with four K-doped rolled W monoblocks provided by the University of Tohoku, Japan.

UT inspections carried out after fabrication show high quality of the joining interface obtained by both HRP and HIP techniques between the CuCrZr pipe and the Cu interlayer. The results after the cyclic thermal fatigue tests at the neutral beam facility GLADIS revealed the formation of discontinuities affecting the HHFT zone of the CuCrZr/Cu interface and of the Cu/W interface as well. For instance, UT results of ENEA80 after 1500 × 20MW/m^2 cycles revealed the presence of debonding, delamination and cracks, without further worsening after the additional 500 cycles. Therefore, it is likely that defects developing during the first 1500 cycles did not grow during the additionally performed 500 cycles. UT inspections of MU II - IJS show the formation of defects at the CuCrZr/Cu interface of the advanced W monoblocks (position 4–5–6) as well as on the Cu/W interface of sintered W monoblocks (position 7–8–9). This last case turned out to be related to cracks in the monoblocks, running almost circumferentially at a depth range of 1–2 mm from the W/Cu interface and extending up to the outer surfaces, as visual inspection confirmed. After the HHFT campaign, UT inspections of MU II - IJS highlighted the formation of discontinuities on monoblocks #9 and #11 (CuCrZr/Cu interface) as well as on monoblock #10 (Cu/W interface). Detailed UT analysis and visual inspection suggest that these defects could be related to a crack propagating in the block up to a depth of 2 mm from the Cu/W interface. Visual inspection confirmed the presence of this crack on the lateral side. As a future outlook, the fabrication of reference blocks with artificial defects is foreseen for each advanced W material. This will allow a more accurate calibration of the measurement system, hence a more precise defect sizing, especially at the level of the Cu/W joining interface and beyond.

CRediT authorship contribution statement

Riccardo De Luca: Writing – original draft, Validation, Methodology, Investigation, Formal analysis, Data curation, Conceptualization, Visualization, Writing – review & editing. **Emanuele Cacciotti:** Writing – original draft, Visualization, Validation, Methodology, Investigation, Formal analysis, Data curation. **Marco Cerocchi:** Writing – review & editing, Visualization, Formal analysis, Data curation. **Francesco Crea:** Writing – review & editing, Supervision, Methodology, Investigation, Formal analysis, Conceptualization. **Selanna Roccella:** Writing – review & editing, Supervision, Resources, Project administration, Methodology, Conceptualization, Funding acquisition, Software, Visualization. **Henri Greuner:** Writing – review & editing, Visualization, Validation, Resources, Project administration, Methodology, Investigation, Data curation, Conceptualization. **Katja Hunger:** Writing – review & editing, Visualization, Validation, Methodology, Investigation, Formal analysis, Resources. **Carsten Bonnekoh:** Writing – review & editing, Visualization, Validation, Supervision, Resources, Project administration, Investigation, Funding acquisition, Conceptualization. **Andrei Galatanu:** Writing – review & editing, Visualization, Validation, Resources, Project administration, Investigation, Conceptualization, Methodology. **Aljaž Iveković:** Writing – review & editing, Visualization, Validation, Resources, Investigation, Conceptualization, Methodology. **Petra Jenuš:** Writing – review & editing, Visualization, Validation, Resources, Investigation, Conceptualization, Methodology. **Marius Wirtz:** Writing – review & editing, Visualization, Supervision, Resources, Project administration, Funding acquisition.

Declaration of competing interest

The authors declare that they have no known competing financial interests or personal relationships that could have appeared to influence the work reported in this paper.

Acknowledgements

This work has been carried out within the framework of the EUROfusion Consortium, funded by the European Union via the Euratom Research and Training Program (Grant Agreement No 101052200 – EUROfusion). Views and opinions expressed are however those of the author(s) only and do not necessarily reflect those of the European Union nor the European Commission can be held responsible for them.

Data availability

Data will be made available on request.

References

[1] F.A J.H. Donnè, The European roadmap towards fusion electricity, Philos. Trans. R. Soc. A: Math., Phys. Eng. Sci. 377 (2141) (2019) 20, 170 432.
[2] T.R. Barrett, et al., Progress in the engineering design and assessment of the European DEMO first wall and divertor plasma-facing components, Fus. En. Des. 109–111 (2016) 917–924.
[3] G. Pintsuk, et al., European materials development: results and perspective, Fus. Eng. Des. 146 (2019) 1300–1307.
[4] M. Rieth, et al., Recent progress in research on tungsten materials for nuclear fusion applications in Europe, J. Nuc. Mat. 432 (2013) 482–500.
[5] S. Wurster, et al., Recent progress in R&D on tungsten alloys for divertor structural and plasma facing materials, J. Nuc. Mat. 442 (2013) S181–S189.
[6] R. Neu, et al., Advanced tungsten materials for plasma-facing components of DEMO and fusion power plants, Fus. Eng. Des. 109–111 (2016) 1046–1052.
[7] D. Terentyev, et al., Development of irradiation tolerant tungsten alloys for high temperature nuclear applications, Nucl. Fusion 62 (2022) 086035, 17pp.
[8] S. Antusch, et al., Processing of complex near-net-shaped tungsten parts by PIM, Nuc. Mat. En. 16 (2018) 71–75.
[9] F. Crea, et al., Mock-ups fabrication by HRP technology with advanced W-alloy monoblocks for DEMO divertor target, Fus. Eng. Des. 201 (2024) 114232.
[10] S. Novak, et al., Beneficial effects of a WC addition in FAST-densified tungsten, Mat. *Sc*. En. A 772 (2020) 138666.
[11] C. Bonnekoh, et al., MAT-T.03.03-T005-D001, Fabrication of mock-ups via HIP. EUROfusion Final Report, EFDA_D_2PVEVT, 2023.
[12] E. Visca, et al., Hot Radial Pressing: an alternative technique for the manufacturing of plasma-facing components, Fus. Eng. Des. 75-79 (2005) 485–489.
[13] H. Greuner, et al., High heat flux facility GLADIS:operational characteristics and results of W7-X pre-series target tests, J. Nuc. Mat. 367-370 (2007) 1444–1448.
[14] T. Minniti, et al., Structural integrity of DEMO divertor target assessed by neutron tomography, Fus. Eng. Des. 169 (2021) 112661.
[15] T. Minniti, et al., Are tungsten-based nuclear fusion components truly invisible to x-ray inspection? Nucl. Fus. 62 (2022) 066003.
[16] C. Pei, et al., Progress on the ultrasonic testing and laser thermography techniques for NDT of tokamak plasma-facing components, Theoret. Appl. Mech. Lett. 9 (2019) 180–187.
[17] S. Roccella, et al., Ultrasonic test results before and after high heat flux testing on W-monoblock mock-ups of EU-DEMO vertical target, Fus. Eng. Des. 160 (2020) 1118.
[18] G. Dose, et al., Ultrasonic analysis of tungsten monoblock divertor mock-ups after high heat flux test, Fus. Eng. Des. 146 (2019) 870–878.
[19] J.-H- You, et al., High-heat-flux performance limit of tungsten monoblock targets: impact on the armor materials and implications for power exhaust capacity, Nuc. Mat. En. 33 (2022) 101307.
[20] S. Roccella, et al., ENEA ultrasonic test on plasma facing units, Fus. Eng. Des. 146 (2019) 2356–2360.